Influence of process parameters on properties of hemp woven reinforcements for composite applications: mechanical properties, bias-extension tests and fabric forming

A.-C. Corbin , D. Soulat, M. Ferreira, and A.-R. Labanieh

ENSAIT, GEMTEX – Laboratoire de Génie et Matériaux Textiles, F-59000 Lille, France

Abstract: Natural fibers are used to produce environmental-friendly composites with good specific mechanical and acoustical properties. Production of woven reinforcement from natural fibers is challenging because of the distinct length of the fibers. A lot of parameters at fiber extraction, spinning and weaving stages have an impact on the composite produced. The purpose of this paper is to study the influence of yarn type and weave diagram on the mechanical properties of woven fabrics, in terms of tensile and shear behavior and deformability at forming. It was observed that weft density is one of the most impacting parameters during forming.

Keywords: natural fibers; woven fabrics; composite reinforcements; mechanical behavior; shear properties; fabric forming

Introduction

The currently growing interest for environmental concerns leads to rethink the production and the raw materials used for composite materials. One alternative is to use natural fibers to replace man-made fibers, in particular thanks to their good thermal and insulation behaviors and their correct specific gravity properties, similar to those of man-made fibers (natural fibers have very low density in comparison to man-made fibers) (Pil et al. 2016; Mohanty et al. 2018). However, natural fibers are discontinuous fibers and cannot be directly used in the weaving process. The production of yarns or rovings allows the alignment of fibers in one direction, while cohesion is obtained by twisting. Although twisting provides the mechanical strength required for the weaving process, it also induces misalignment of fibers (fibers are less oriented in yarn direction) and impregnations defects (it is more difficult for the resin to penetrate in the core of the yarns and of the fibers) (Omrani, et al. 2017; Shah, Schubel, and Clifford 2013). Rovings can be used as an alternative totwisted yarn. They are assemblies of aligned fibers but with a lesser twist level and with more fiber density in cross section (Baley et al. 2018; Omrani et al. 2017). An improvement of rovings strength is commonly done by chemical method (such as chemical treatment or addition of binding agents) to achieve the strength required for weaving process (Matykiewicz et al. 2019; Sepe et al. 2018).

Nonwoven and unidirectional reinforcement are preferred for the manufacturing of natural fibers composites because they allow to achieve sufficient mechanical properties with a reduced cost of raw materials (Shah 2014). However, for applications which require high loads, woven fabrics reinforcements need to be produced with continuous fibers (Pil et al. 2016; Baley et al. 2018; Bourmaud et al. 2018). For unidirectional fabrics, mechanical properties are high in the direction of the tapes, and very weak or even nulin transverse direction. With nonwoven fabrics, due to the manufacturing process and the anisotropy of fiber distribution, properties are different in the two main directions, and often better in the machine direction (MD). Even if this kind of reinforcements is cheaper than woven fabrics, their main defect occurs during manufacturing of composite parts: the handling and preforming of nonwoven or unidirectional preforms lead to variations of fiber density, and maybe holes, or spacing between the tapes in areas where high deformations are applied (Baley et al. 2018; Omrani et al. 2017). Woven fabrics are made of yarns or rovings in the two main directions, so their mechanical properties are better in both directions than with unidirectional or nonwoven fabrics. Moreover, by using woven fabrics as reinforcements, it is possible to control the deformability of the preform during composite manufacturing process. During forming process, defects may occur, like sliding or buckles of yarns, but they are less significant than with nonwovens. Handling of woven fabrics during composite manufacturing process is also easier, because the structure is more stable (Baley et al. 2018; Capelle et al. 2014; Pil et al. 2016).

A lot of studies about natural fibers (Haag et al. 2017; Kabir et al. 2013; Placet et al. 2018) or composites reinforced by natural fibers (Baley et al. 2018; Shahzad 2012; Torres et al. 2017) have been previously conducted in the literature. However, only few studies are available with several kinds of reinforcements, and their properties are often only evaluated at composite scale (Torres et al. 2017; Rajesh, Singh, and Pitchaimani 2018; Khan et al. 2016). In order to manufacture composites materials with as few defects as possible, it is necessary to understand the behavior of the reinforcement used at dry state. During composite manufacturing processes, reinforcement fabrics undergo many types of solicitations, such as tension and shear. Specific tests have been developed for composites reinforcement to study the in-plane shearing behavior, through uniaxial bias-extension test (Boisse et al. 2017; Cao et al. 2008), and the deformability, with preforming tests (Omrani et al. 2017; Jacquot et al. 2016), but these studies were mainly conducted with man-made fibers.

In this study, four composites reinforcements are manufactured by weaving technology using flax and hemp fibers. These woven fabrics have different process parameters, such as type of yarn used, weave diagrams and weft densities. The influence of these process parameters is studied through tensile tests, shearing behavior (with bias-extension tests) and forming test. According to the type of yarns or the weave diagrams, several tendencies are observed. Once these properties are listed, it is possible to choose the best process parameters to produce reinforcements with properties optimized for the final composite application.

Materials

Twisted yarns and rovings

Flax and hemp fibers, in the form of twisted yarns and rovings supplied by an Italian Company, Linificio e Canapficio Nazioanle, are used to manufacture woven reinforcements for biobased composites. Their properties are shown in **Erreur ! Source du renvoi introuvable.**. As commonly used in textile industry, a conventional chemical treatment is done to the rovings to improve their mechanical properties and thus their weavability. A previous study (Corbin et al. 2018) shown that this kind of treatment improves weavability of rovings without damaging the fibers and composites properties. For these three types of yarns, linear density is measured according to the standard NF G07-316, twist level according to the standard NF G07-079 and tenacity at break according to the standard NF EN ISO 2062.

The flax twisted yarn has a lower linear density, which means it has less fibers per unit length, and higher twist level. Rovings have higher linear density, and thus more fibers on the cross-section, and lower twist level than twisted yarns. However, the flax rovings used in this study did not have the required strength to endure the preparations steps of weaving process, so that twisted yarns flax were also used to manufacture composite reinforcements.

Table 1: Yarns properties

Yarn	Linear density (Tex)	Twist level (turns/m)	Tenacity at break (cN/Tex)
Flax twisted yarn	173 ± 14	231 ± 18	25.3 ± 3.4
Flax roving	334 ± 26	32 ± 4	5.2 ± 1.1
Hemp roving	259 ± 10	36 ± 3	24.2 ± 3.7

Preforms

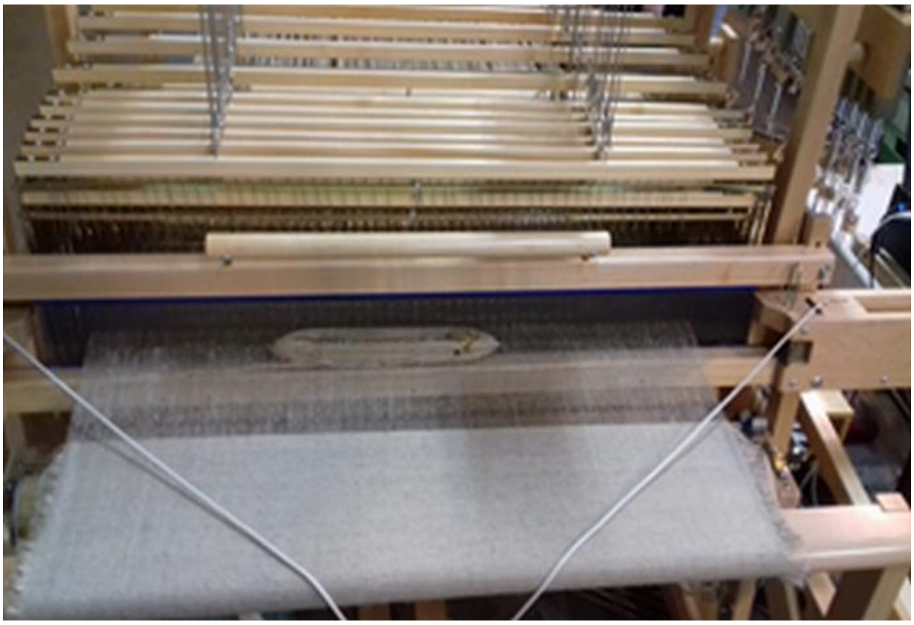

Figure 1: Manual weaving machine

With the flax and hemp yarns presented in **Erreur ! Source du renvoi introuvable.**, four woven fabrics are produced on a manual weaving machine at ENSAIT laboratory visible on **Erreur ! Source du renvoi introuvable.**. **Erreur ! Source du renvoi introuvable.** presents the woven fabrics produced and their main properties in terms of yarn types, yarn densities, areal densitiy, thickness and air permeability. **Erreur ! Source du renvoi introuvable.** presents 3D views (with warp yarns in blue and weft yarns in red) and schemas of the three weave diagram used, made with WiseTex® software) and also pictures of the four woven fabrics produced. Areal density is evaluated according to the standard NF EN 12127, thickness according to the standard NF EN ISO 5084 and air permeability according to the standard NF EN ISO 9237. One fabric is woven with flax fibers and three with hemp fibers, with the same warp density of 6 yarns/cm. Thus, one fabric has twisted yarns in warp direction and rovings in weft direction (FPW woven fabric) and three fabrics have rovings in both directions (HPW, HSA and HTW woven fabrics), which allow studying the influence of the yarns type on fabric properties. For hemp fabrics, three different weave diagrams, plain weave diagram for HPW fabric, satin weave diagram for HSA fabric and twill 6 weave diagram for HTW fabric are chosen to analyze the impact of weave diagram on reinforcements' behavior. Satin 6 and twill 6 weave diagrams have less binding points (interlacements between warp and weft yarns, black squares on representations of **Erreur ! Source du renvoi introuvable.**) than plain weave diagram, which results in higher weft densities in HSA and HTW woven fabrics in comparison to FPW and HPW. This increase in weft densities leads to higher thickness and areal density for HSA and HTWin comparison to FPW and HPW. All fabrics have the same warp density of 6 yarns/cm, the obtained weft density is varied with full-packing the ability inserted weft yarns on weaving loom. The measured weft densities for each fabric out of machine are shown in **Erreur ! Source du renvoi introuvable.** summarizing all weaving parameters of hemp and flax fabrics. The satin and twill weave, characterized by less waviness and crossing of constitutive yarns comparing with plain weave, lead to obtain higher weft packing and density. This results in higher thickness and areal density for satin (HSA) and twill (HTW) in comparison with plain weave fabrics (HPW and FPW). For the same weave diagram, the use of twisted yarns, which have lower diameter due to the high twist level applied, instead of rovings in warp direction (FPW) induces a thickness slightly lower than with the use of roving in this direction (HPW). This smaller circumference for twisted yarn induces also more spaces between yarns than in other preforms made with rovings in both directions. Thus, it is easier for the air to pass through FPW woven fabric, and its air permeability (1935 L/m²/s) is three times higher than HPW, HSA and HTW woven fabrics (respectively 756, 401 and 670 L/m²/s). For preforms with hemp rovings in both directions, air permeability depends on alignment of binding points, which varies according to the weave diagram (**Erreur ! Source du renvoi introuvable.**). With plain weave diagram, there is a lot of binding points among the fabric, which creates a lot of possibilities for the air to pass through the fabrics and HPW has the higher air permeability for the woven fabrics made of hemp rovings. For satin and twill weave diagrams, the number of binding points per weave repeat is the same, but they are arranged in staggered row for satin and in diagonal for twill. As, it is easier for the air to pass through the fabric along the diagonal, air permeability is higher for HTW than for HSA.

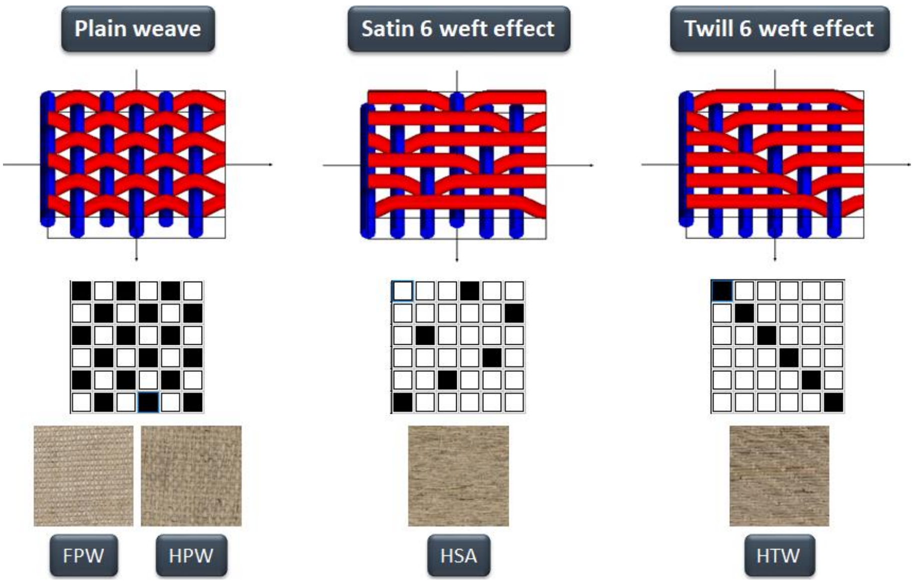

Figure 2: Representations of weave diagrams

Table 2: Woven fabrics properties

Preform	FPW	HPW	HSA	HTW
Weave diagram	Plain weave	Plain weave	Satin 6	Twill 6
Warp yarns	Flax twisted yarn	Hemp roving	Hemp roving	Hemp roving
Weft yarns	Flax roving	Hemp roving	Hemp roving	Hemp roving
Warp density (yarns/cm)	6	6	6	6
Weft density (yarns/cm)	5.8	5	9.5	9.5

Areal density (g/m²)	288 ± 20	278 ± 8	426 ± 8	402 ± 3
Thickness (mm)	0.91 ± 0.03	0.98 ± 0.07	1.55 ± 0.05	1.59 ± 0.06
Air permeability (L/m²/g)	1935 ± 219	756 ± 78	401 ± 46	670 ± 115

Characterization steps

Tensile properties

The tensile tests of woven fabrics are conducted according to the standard NF EN ISO 13934-1 on an MTS Criterion 45 tensile machine. Fives samples are cut in each main direction of the woven fabrics (five in warp direction and five in weft direction), with a length of 300 mm and a width of 50 mm. During the tensile test, the gauge length is 200 mm, the crosshead displacement rate is 20 mm/min and a preload of 5N is applied. Sandpapers are used inside the jaws of the tensile machine to avoid slippages of thetest specimen. Tensile parameters studied are maximal load and strain at maximal load, which is compared with shrinkages measured according to the standard NF EN ISO 7211-3.

In-plane shear properties

Figure 3 near here

In order to evaluate the behavior of woven fabrics under shear stresses, uniaxial bias-extension (UBE) tests are performed. Uniaxial bias-extension tests are widely used to study the in-plane shear properties of glass or carbon woven fabrics (Boisse et al. 2017; Cao et al. 2008). Shearing behavior differs according to dimensions of the sample, as mentioned on Figure 3.a. The evolution of the UBE test at three different moments during the test is shown in Figure 3.b. During the test, the extension of the sample leads to an extension of zones B and C and a shearing behavior between the yarns of these two zones. Samples are cut in woven fabrics at 45°, with a length of 250 mm and a width of 50 mm, so the ratio L/l is higher than 2. The test is conducted on a MTS Criterion 45 tensile machine with a gauge length of 150 mm, a crosshead displacement rate of 20 mm/min, no preload and sandpapers inside the jaws to avoid slippage. A video recording is used to measure the shear angle between warp and weft yarns during the entire test. Measured shear angles are compared with theoretical shear angle, calculated with Equation (1). Normalized shear force is calculated according to Equation (2) to compare the in-plane shear behavior of woven fabrics between them.

$$\gamma_{th} = \frac{\pi}{2} - 2cos^{-1}\left(\frac{\sqrt{2}}{2}\left(1 + \frac{d}{L-l}\right)\right) \qquad (1)$$

$$F_{sh} = \frac{FD}{l(2D-l)\cos\gamma}\left(\cos\frac{\gamma}{2} - \sin\frac{\gamma}{2}\right) - \frac{l\cos^{\gamma}/_{2}}{(2D-l)\cos\gamma}F_{sh}\left(\frac{\gamma}{2}\right) \qquad (2)$$

With γ_{th}: theoretical shear angle

d: displacement of the tensile machine

L: gauge length

l: width of the sample

Fsh: normalized shear force

F: force recorded by the tensile machine

D: length of the pure in-plane shear zone (zone C)

γ: shear angle (measured on pictures)

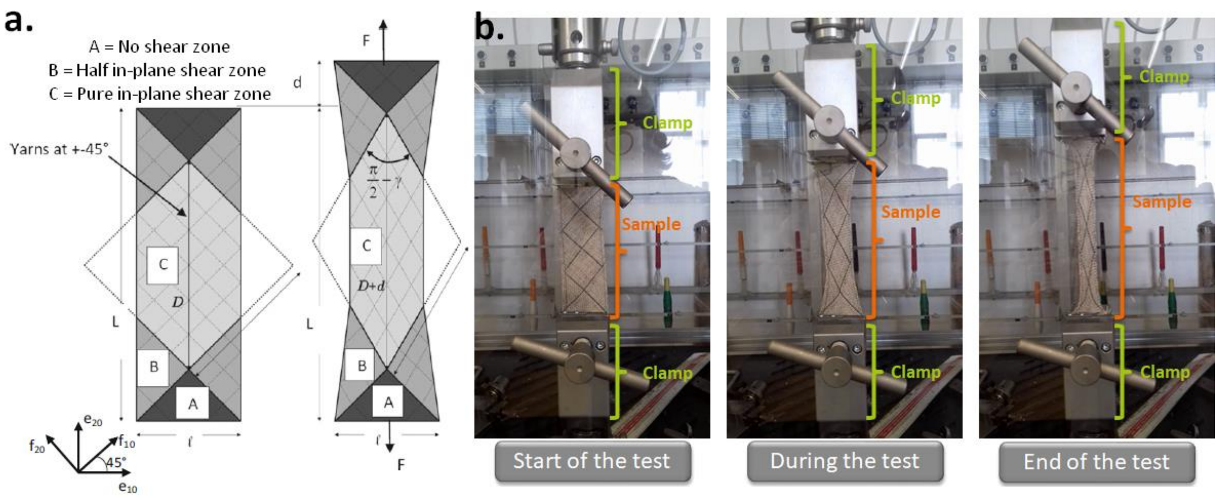

Figure 4: UBE tests samples a. description of shear zones (Boisse et al. 2017) b. evolution of sample during the test

Fabric forming

Fabric forming tests are performed on a specific device developed at ENSAIT laboratory (Omrani et al. 2017) and visible on **Erreur ! Source du renvoi introuvable.**.a. and **Erreur ! Source du renvoi introuvable.**.b. During preforming of the woven fabrics, tensile and shear stresses are applied to the reinforcement at the same time, which simulates composite manufacturing process, and drapability of the fabric can be analyzed. The punch shape used is a hemispherical shape with a diameter of 150 mm, the set-upis presented in **Erreur ! Source du renvoi introuvable.**.c. The punch speed is constant and cannot be changed, with a value of 45 mm/s and the blank-holder pressure applied is 0.2 MPa. For this study, only one layer of fabric is placed on the preforming device, always withthe same orientation. Three parameters are studied to characterize the forming behavior of the fabrics. The first one is the preforming load required to give the shape of the punch to the fabric, which is measured with a load sensor located under the punch. The second one is the material draw-in, measured along the fabric on one side in warp direction and on another side in weft direction, which shows the fabric consumption needed to fit closely with the punch shape. Finally, the third parameter is the shear angle between yarns, measured on a picture taken at the end of the test on several locations on the fabrics. Areas with similar shear angles are then created to assist in the analysis.

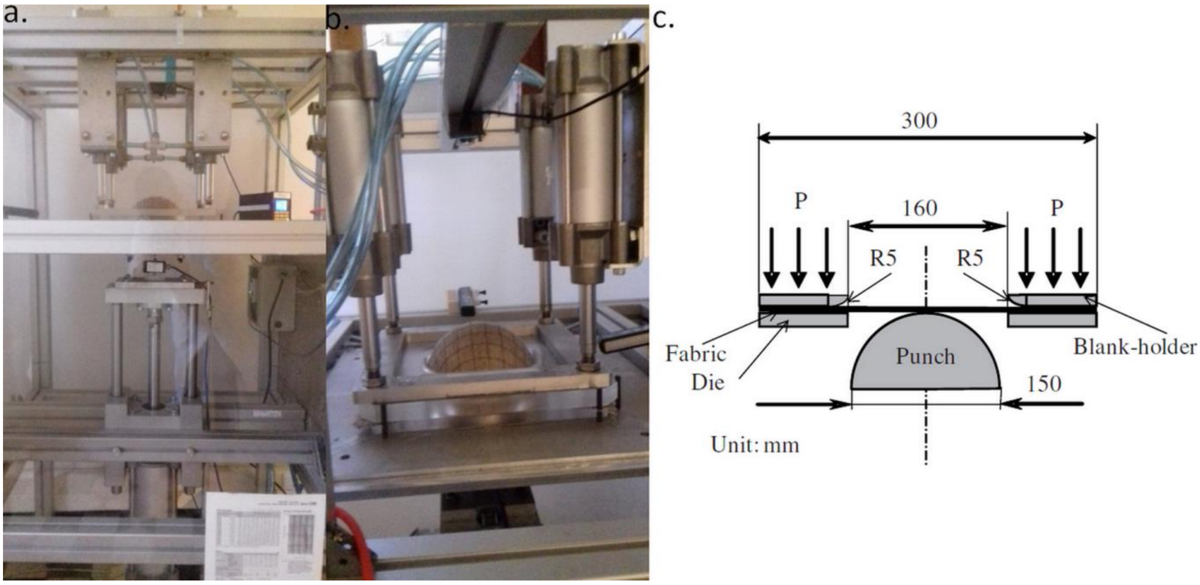

Figure 5: Preforming tests a. and b. Pictures of preforming device c. Principle of preforming device

Results and discussion

Mechanical properties

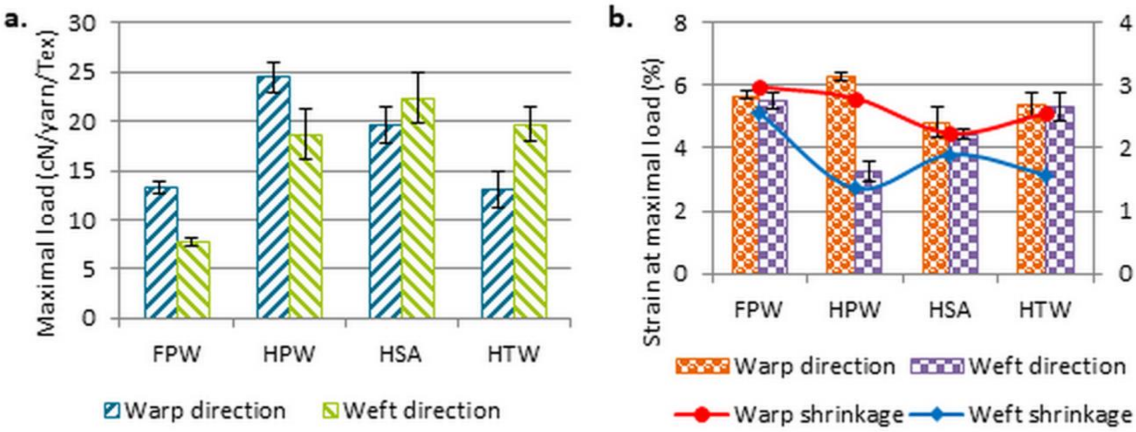

Figure 6: Tensile properties of woven fabrics a. Maximal load b. Strain at maximal load and shrinkages

The maximal load, in **Erreur ! Source du renvoi introuvable.**.a., is presented in cN/yarn/Tex to avoid effects of yarns densities and linear density of yarns used. The three hemp fabrics (HPW, HSA and HTW) have better maximal load than flax fabric

(FPW) in weft direction. That is attributed to the low tenacity of the flax roving, as shown in **Erreur ! Source du renvoi introuvable.**, in the weft direction of flax fabric FPW in comparison with hemp roving. In warp direction flax fabric FPW has higher maximal load than in weft direction for the same reason of low tenacity of flax rovings in comparison with flax yarns, as shown in **Erreur ! Source du renvoi introuvable.**. In warp direction of FPW, even if warp density is the same for all the fabrics studied, the yarns used have a linear density 1.5 times lower than rovings used in warp direction in other fabrics (see **Erreur ! Source du renvoi introuvable.**). Indeed, there are fewer fibers in section for FPW fabric in warp direction, which leads to lower maximal load. However, flax and hemp fabrics manufactured with plain weave diagram (FPW and HPW) exhibits lower maximal loads in comparison with hemp fabrics with satin and twill weave diagram (HSA and HTW).

The tensile response of the hemp fabrics HPW, HSA and HTW in both directions is influenced by the used weave diagram. HSA fabric has balanced maximal load between the both directions, whereas maximal load is higherin warp direction for HPW and in weft direction for HTW. In this way, it is possible to choosethe weave diagram depending on the properties wanted for the reinforcement. Values of strain at maximal load and shrinkages, illustrated on **Erreur ! Source du renvoi introuvable.**.b. follow the same trend. Strain of the woven structure is correlated to the crimp of yarns inside the fabric: under an applied load, waved yarns firstly are redressed and then, once extended in load direction, they resist to the applied load. Thus the first phase of strain-load curve of fabric under uniaxial loading is strongly dependant of yarn shrinkage. However, yarn shrinkage induces fibre misalignment, which involves lower mechanical properties for composites (Rayyaan et al. 2020).. Both strain at maximal load and shrinkage values are higher in warp direction than in weft direction. That is attributed to the weaving process. When the weaving reed is refolded during weaving process, the warp yarns are forced to undulate inside the woven fabrics, which create important warp shrinkage. In the case of weft direction, as the warp density is not so high regarding conventional textile industry, weft yarns tend to remain straight inside the woven fabrics, which lead to a poor weft shrinkage.

Shear properties

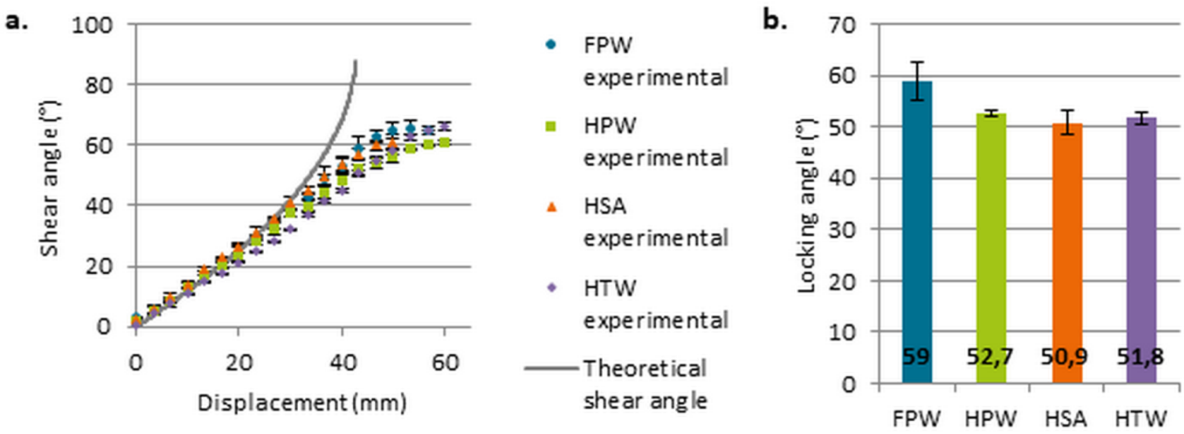

Figure 7: Shear angle - displacement (UBE test)

On the “shear angle – displacement” curve (**Erreur ! Source du renvoi introuvable.**.a.), theoretical and experimental in-plane shear behaviors are compared. According to the literature (Boisse et al. 2017), the in-plane shear locking angle is considered to be reached when the two curves split, and beyond this value, the specimen is not considered to be in pure shear any more (slippage or wrinkles) (Pourtier et al. 2019). These values are reported in **Erreur ! Source du renvoi introuvable.**.b. Two kinds of comparisons can be made: according to the type of used yarn and according to the number and placement of binding points. First, for fabrics with the same type of yarns in both directions (fabrics made with hemp rovings), the locking angle is higher for plain weave diagram (HPW), then for twill weave diagram (HTW) and finally for satin weave diagram (HSA). Further, the placement of binding points, FPW and HPW have one binding point everytwo yarns whereas HSA and HTW have one binding point everysix yarns (**Erreur ! Source du renvoi introuvable.**). In twill weave diagram, there is diagonal alignment of binding points and four contact points between floats (schematized by orange dotted lines in **Erreur ! Source du renvoi introuvable.**). With this placement, there are more possibilities for deformation of the fabric, the alternative of 2-2 contact points (blue dotted lines in **Erreur ! Source du renvoi introuvable.**) and 3-1 contact points (green dotted lines) in satin weave diagram giving more stability to the fabric. Thus, HTW woven fabric has a higher locking angle than HSA woven fabric. With plain weave diagram, the symmetrical placement of binding points leads to better deformability in shearing, which induces higher locking angle for FPW and HPW woven fabrics.

When the weave diagram is the same but the type of used yarn in warp direction is different, the fabric having higher space between yarns as for FPW exhibits higher locking angle in comparison with fabric having less space between roving in HPW. This effect can be highlighted through the comparison of the locking angle i with air permeability, in

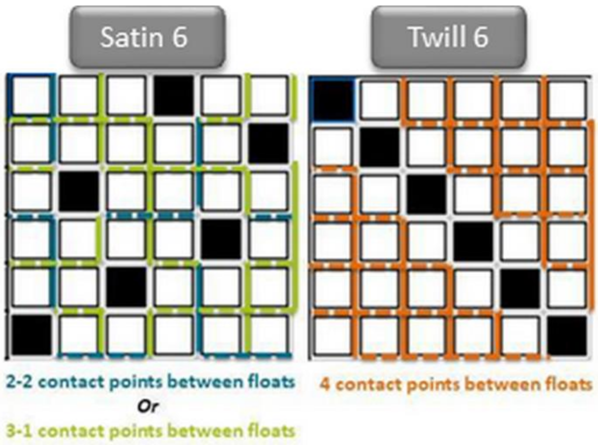

Figure 8: Contacts points between floats in satin 6 and twill 6 weave diagrams

. The air permeability of fabric permits to distingue between fabrics regarding the inter-yarn space. Higher permeability level indicates bigger space between yarns resulting in higher shear locking angle. That explains the highest shear locking angle for

FPW fabric, which is made of twisted yarns in warp direction and rovings in weft direction, having highest permeability level.

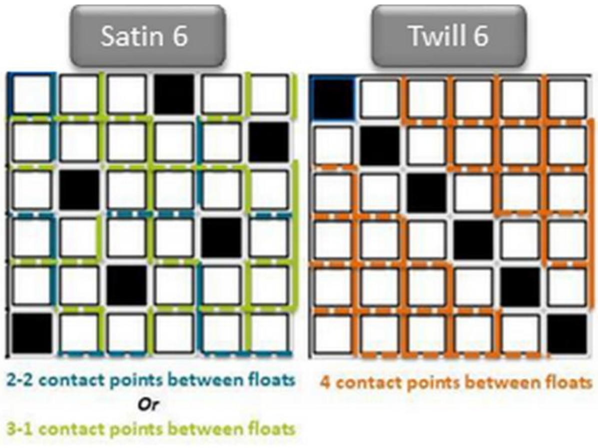

Figure 8: Contacts points between floats in satin 6 and twill 6 weave diagrams

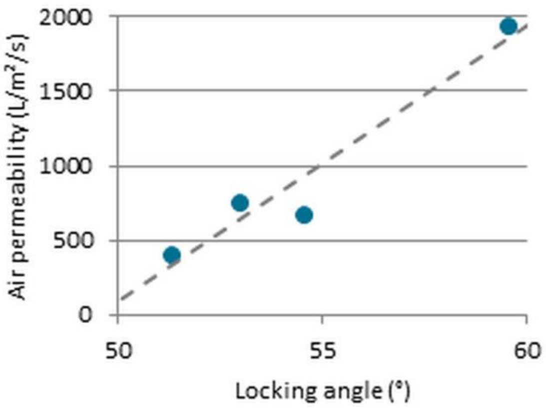

Figure 9: Comparison between locking angle (UBE test) and air permeability

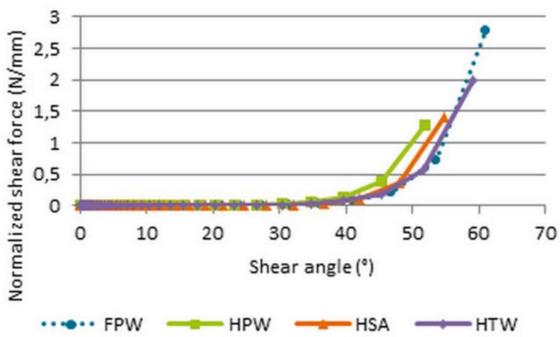

Figure 10: Normalized shear force (UBE test)

The normalized shear force for each fabric (Equation (2)) is drawn in

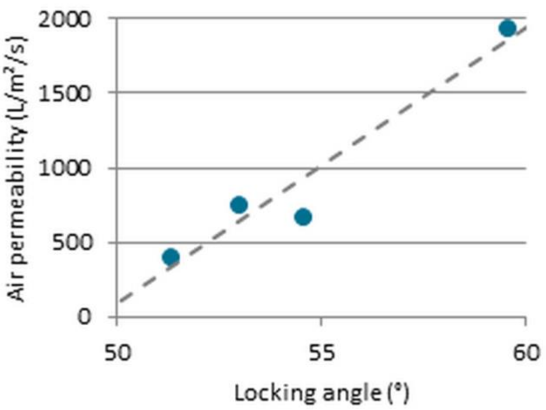

Figure 9: Comparison between locking angle (UBE test) and air permeability

. For all the woven fabrics studied, the behavior is similar, no trend emerges. For the fabric with twisted yarns in one direction and rovings in other direction (FPW), the normalized shear force is slightly higher. As FPW has also a locking angle slightly higher than the other fabrics, the use of twisted yarns in one direction and rovings in other direction can be used to manufacture reinforcement with better in-plane shear properties permitting better fitting with more complicated curved shape.

Fabric forming

During fabric forming on the hemispherical punch, no defects, as wrinkles, buckles (Ouagne et al. 2013; Capelle et al. 2014) or intra-ply sliding (Labanieh et al. 2018), occurs for all fabrics These types of defects were described for more complex shapes (Wang et al., 2015), or for hemispherical punch shape but for 45° orientation fabric (Labanieh et al., 2018). During the test, woven fabric conforms to the punch shape, which results in draw-in on the edges of the sample. Values of draw-in along these edges are measured for each fabric and reported in **Erreur ! Source du renvoi introuvable.**. For both directions, the trend is similar between all the reinforcements studied. For 0/90° orientation of fabric, relatively to the shape, draw-in is null in the corners and gradually increases to the middle of the sample. On this shape , all the woven preforms have good deformability capability: they adapt well to the punch shape around the impact point.

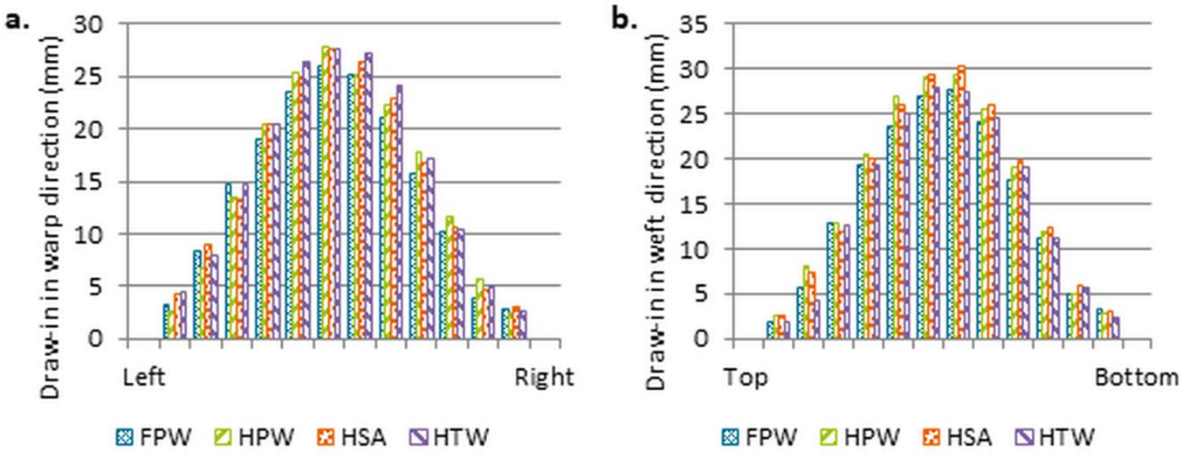

Figure 11: Draw-in of woven fabrics during forming test a. Warp direction b. Weft direction

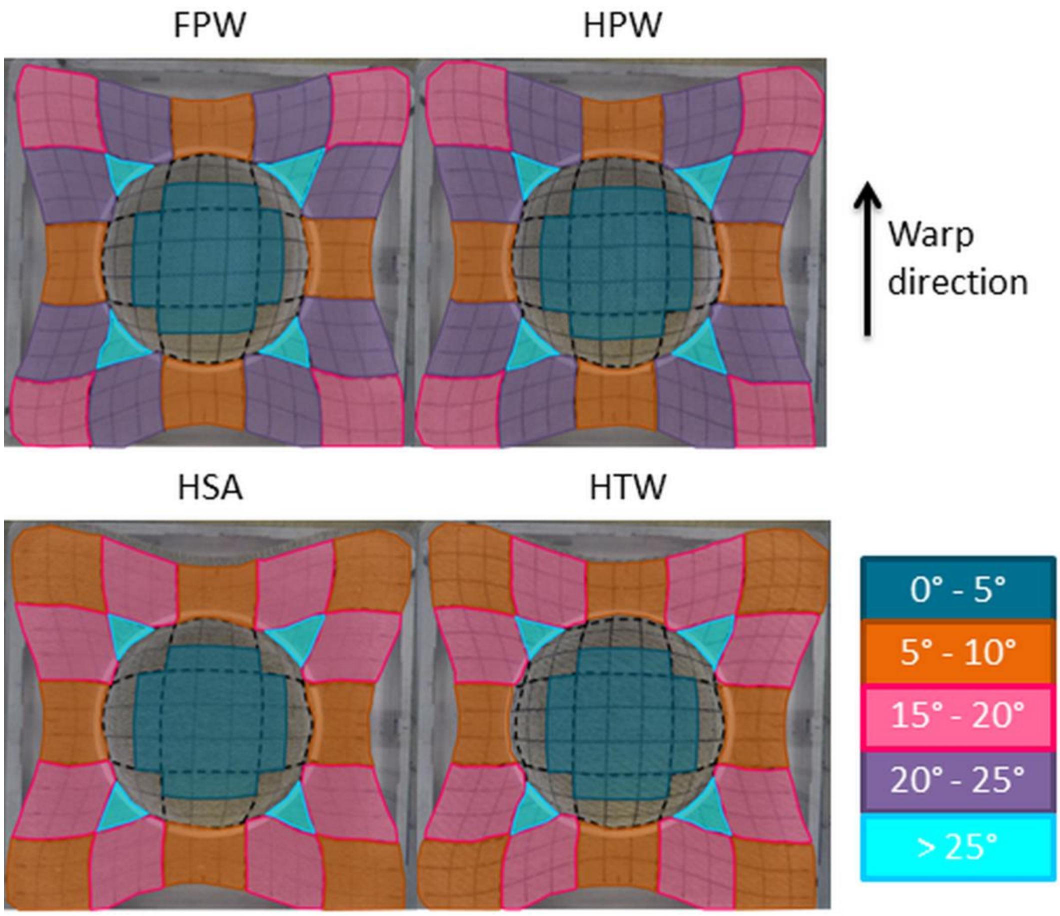

Figure 12: Shear angles during preforming test

Shear angles measured during forming tests are presented in

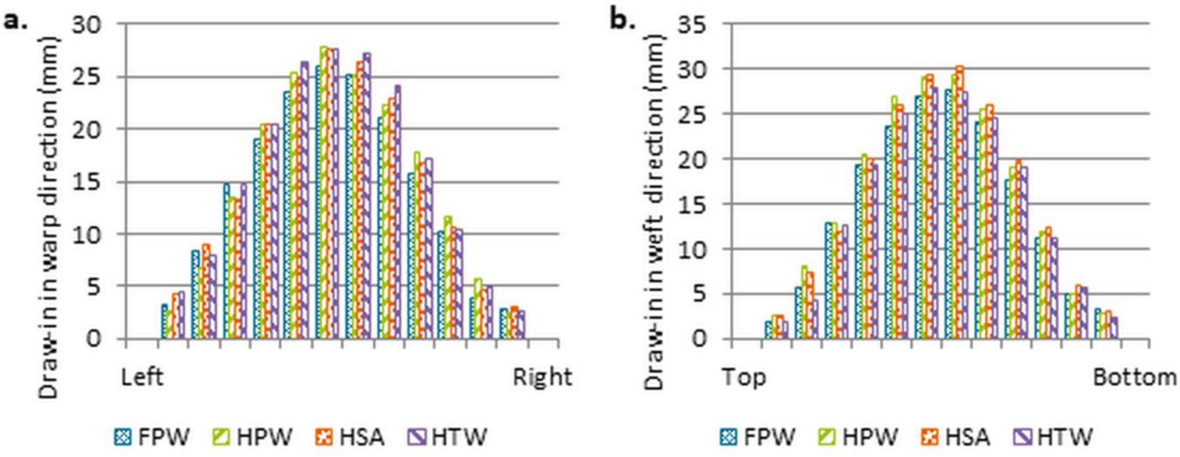

Figure 11: Draw-in of woven fabrics during forming test a. Warp direction b. Weft direction

. Maximum sheared zones are at the base of the hemisphere (blue area). There is a similar behavior between plain weave diagram (FPW and HPW) and another similar behavior between satin and twill weave diagrams. Thus, the number of biding points (18 per 6 x 6 yarns area in plain weave diagram whereas only 6 per 6 x 6 yarns area in satin or twill) influences the shear behavior of the woven fabrics. Shear is gradual and smoother in satin and twill weave diagram in comparison with plain weave diagram. With these measurements of shear angles, maximal shear angles are determined in **Erreur ! Source du renvoi introuvable.** (as an average of values in the corners of the punch shape). For forming test, maximal shear angle is similar for all fabrics satin and plain weave diagrams (FPW, HPW and HSA fabrics) and lower for twill weave diagram (HTW). The binding points arranged in staggered rows give more deformability to the woven fabrics. These shear angles remains lower than locking angles values identified during UBE tests which may explain the absence of wrinkle-type defects or inhomogeneity of material density after forming.

Table 3: Maximal shear angle (forming test)

Preform	Maximal shear angle (°)
FPW	35.3 ± 2.9
HPW	37.0 ± 0.8
HSA	35.2 ± 0.5
HTW	33.8 ± 1.3

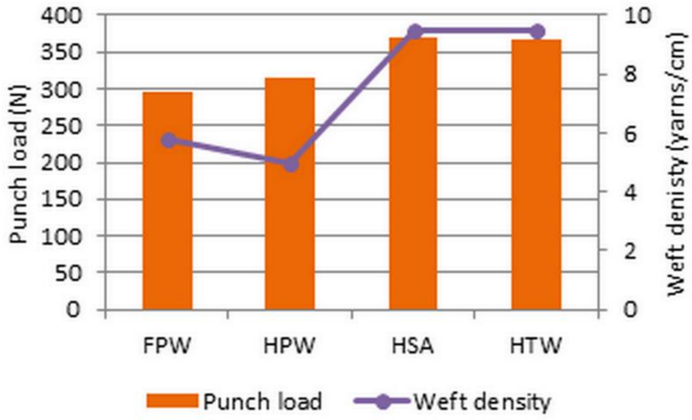

Figure 13: Punch load (forming test)

The punch load at the end of the test, recorded by the load sensor of the forming device, is presented in Table 3: Maximal shear angle (forming test)

Preform	Maximal shear angle (°)
FPW	35.3 ± 2.9
HPW	37.0 ± 0.8
HSA	35.2 ± 0.5
HTW	33.8 ± 1.3

for all fabrics and compared with their respective weft densities. As for shear angles, FPW and HPW have similar behavior whereas HSA and HTW have another similar behavior. The punch load is 1.2 times higher for HSA and HTW fabrics, which also have higher weft density and higher areal density (table 1). As explained previously, this increase of weft densities lead to higher fiber content in the fabrics and consequently an increasing of the forming load. Further, the higher fiber content is associated with higher roughness inducing higher friction loads on fabrics which slides on the die and blank holder surfaces causing higher forming load.

Conclusion

The knowledges of the woven process and of the influence of process parameters on woven fabrics properties allow to produce reinforcements which meetwith composite applications requirements. In this study, two main process parameters have been studied: the influence of the type of yarn and the weave diagram. Tensile properties of woven fabrics depend on these production parameters: reinforcements can have balanced or unbalanced property between warp and weft directions in terms of the maximal load, and can be more or less extensible in both main directions, due to shrinkage of yarns inside the woven fabric. However, an important shrinkage leads to misalignments of fibers in both main directions. The final shape of composite materials are often complex, and reinforcements are formed into the desired shape in the dry state. The reinforcement formability, to fit the desired shape without inducing structural defects, depends essentially on its shear deformability. Thus, uniaxial bias-extension test have been performed to study shear properties of woven fabrics, and preforming tests have been conducted to study tensile and shear properties in the same time. Under a shear load, the behavior of the woven fabrics mainly depends on space available between the yarns, which is induced by the type of the yarn and the arrangement of interlacement points according to the chosen weave diagram. The air permeability of the fabric has been used as an indicator of the inter-yarn space. Finally, with preforming tests, woven preforms have been submitted to both tensile and shear loads at the same time. Behavior of woven fabrics during preforming tests varies according to the type of yarns and the weave diagram used, and also more specifically according to the weft density, which tends to stiffen the woven fabric when it is important. Therefore, by choosing process parameters and especially the type of yarns used and the weave diagram, it is possible to develop woven preforms which fit with final composites applications requirements.

Acknowledgments

The authors would like to thank the Italian Company "Linificio e Canapificio Nazionale" for providing twisted yarns and roving used in this study. This project has received funding from the Bio Based Industries Joint Undertaking under the European Union's Horizon 2020 research and innovation program under the grand agreement no. 744349.

Funding

This work was supported by the Horizon 2020 Framework Programme [744349].

ORCID

A.-C. Corbin http://orcid.org/0000-0003-1542-9689

References

Baley, C., M. Gomina, J. Breard, A. Bourmaud, S. Drapier, M. Ferreira, A.L. Duigou, et al. 2018. Specific Features of Flax Fibres Used to Manufacture Composite Materials. *International Journal of Material Forming* (December 18): 1–30.

Boisse, P., N. Hamila, E. Guzman-Maldonado, A. Madeo, G. Hivet, and F. dell'Isola. 2017. The Bias-Extension Test for the Analysis of in-Plane Shear Properties of Textile Composite Reinforcements and Prepregs: A Review. *International Journal of Material Forming* 10, no. 4 (August): 473–492. http://link.springer.com/10.1007/s12289-016-1294-7.

Bourmaud, A., J. Beaugrand, D.U. Shah, V. Placet, and C. Baley. 2018. Towards the Design of High-Performance Plant Fibre Composites. *Progress in Materials Science* 97 (August 1): 347–408. http://www.sciencedirect.com/science/article/pii/S0079642518300653.

Cao, J., R. Akkerman, P. Boisse, J. Chen, H.S. Cheng, E.F. de Graaf, J.L. Gorczyca, et al. 2008. Characterization of Mechanical Behavior of Woven Fabrics: Experimental Methods and Benchmark Results. *Composites Part A: Applied Science and Manufacturing* 39, no. 6 (June 1): 1037–1053. http://www.sciencedirect.com/science/article/pii/S1359835X08000572.

Capelle, E., P. Ouagne, D. Soulat, and D. Duriatti. 2014. Complex Shape Forming of Flax Woven Fabrics: Design of Specific Blank-Holder Shapes to Prevent

Defects. *Composites Part B: Engineering* 62 (June 1): 29–36. http://www.sciencedirect.com/science/article/pii/S1359836814000845.

Corbin, A.-C., D. Soulat, M. Ferreira, A.-R. Labanieh, X. Gabrion, and V. Placet. 2018. Multi-Scale Analysis of Flax Fibres Woven Fabrics for Composite Applications. *IOP Conference Series: Materials Science and Engineering* 406, no. 1. https://doi.org/10.1088%2F1757-899x%2F406%2F1%2F012016.

Haag, K., J. Padovani, S. Fita, J.-P. Trouvé, C. Pineau, S. Hawkins, H. De Jong, et al. 2017. Influence of Flax Fibre Variety and Year-to-Year Variability on Composite Properties. *Industrial Crops and Products* 98, no. Supplement C (April 1): 1–9. http://www.sciencedirect.com/science/article/pii/S0926669016308585.

Jacquot, P.-B., P. Wang, D. Soulat, and X. Legrand. 2016. Analysis of the Preforming Behaviour of the Braided and Woven Flax/Polyamide Fabrics. *Journal of Industrial Textiles* 46, no. 3 (September 1): 698–718. https://doi.org/10.1177/1528083715591592.

Kabir, M.M., H. Wang, K.T. Lau, and F. Cardona. 2013. Tensile Properties of Chemically Treated Hemp Fibres as Reinforcement for Composites. *Composites Part B: Engineering* 53, no. Supplement C (October 1): 362–368. http://www.sciencedirect.com/science/article/pii/S1359836813003028.

Khan, G.M.A., M. Terano, M.A. Gafur, and M.S. Alam. 2016. Studies on the Mechanical Properties of Woven Jute Fabric Reinforced Poly(l-Lactic Acid) Composites. *Journal of King Saud University - Engineering Sciences* 28, no. 1 (January 1): 69–74. http://www.sciencedirect.com/science/article/pii/S1018363913000548.

Labanieh, A.R., C. Garnier, P. Ouagne, O. Dalverny, and D. Soulat. 2018. Intra-Ply Yarn Sliding Defect in Hemisphere Preforming of a Woven Preform. *Composites Part A: Applied Science and Manufacturing* 107 (April 1): 432–446. http://www.sciencedirect.com/science/article/pii/S1359835X18300186.

Matykiewicz, D., M. Barczewski, O. Mysiukiewicz, and K. Skórczewska. 2019. Comparison of Various Chemical Treatments Efficiency in Relation to the Properties of Flax, Hemp Fibers and Cotton Trichomes. *Journal of Natural Fibers* (August 9).

Mohanty, A.K., S. Vivekanandhan, J.-M. Pin, and M. Misra. 2018. Composites from Renewable and Sustainable Resources: Challenges and Innovations. *Science* 362, no. 6414 (November 2): 536–542. http://science.sciencemag.org/content/362/6414/536.

Omrani, F., P. Wang, D. Soulat, and M. Ferreira. 2017. Mechanical Properties of Flax-Fibre-Reinforced Preforms and Composites: Influence of the Type of Yarns on Multi-Scale Characterisations. *Composites Part A: Applied Science and Manufacturing* 93, no. Supplement C (February 1): 72–81. http://www.sciencedirect.com/science/article/pii/S1359835X16303943.

Omrani, F., P. Wang, D. Soulat, M. Ferreira, and P. Ouagne. 2017. Analysis of the Deformability of Flax-Fibre Nonwoven Fabrics during Manufacturing. *Composites Part B: Engineering* 116 (May 1): 471–485. http://www.sciencedirect.com/science/article/pii/S1359836816304036.

Ouagne, P., D. Soulat, J. Moothoo, E. Capelle, and S. Gueret. 2013. Complex Shape Forming of a Flax Woven Fabric; Analysis of the Tow Buckling and Misalignment Defect. *Composites Part A: Applied Science and Manufacturing* 51 (August 1): 1–10. http://www.sciencedirect.com/science/article/pii/S1359835X13000997.

Pil, L., F. Bensadoun, J. Pariset, and I. Verpoest. 2016. Why Are Designers Fascinated by Flax and Hemp Fibre Composites? *Composites Part A: Applied Science and Manufacturing* 83, no. Supplement C. Special Issue on Biocomposites (April 1): 193–205. http://www.sciencedirect.com/science/article/pii/S1359835X15004017.

Placet, V., C. François, A. Day, J. Beaugrand, and P. Ouagne. 2018. Industrial Hemp Transformation for Composite Applications: Influence of Processing Parameters on the Fibre Properties. In *Advances in Natural Fibre Composites*, 13–25. R. Fangueiro and S. Rana Eds. https://doi.org/10.1007/978-3-319-64641-1_2.

Pourtier, J., B. Duchamp, M. Kowalski, P. Wang, X. Legrand, and D. Soulat. 2019. Two-Way Approach for Deformation Analysis of Non-Crimp Fabrics in Uniaxial Bias Extension Tests Based on Pure and Simple Shear Assumption. *International Journal of Material Forming* (March 29). https://doi.org/10.1007/s12289-019-01481-8.

Rajesh, M., S.P. Singh, and J. Pitchaimani. 2018. Mechanical Behavior of Woven Natural Fiber Fabric Composites: Effect of Weaving Architecture, Intra-Ply Hybridization and Stacking Sequence of Fabrics. *Journal of Industrial Textiles* 47, no. 5 (January): 938–959. http://journals.sagepub.com/doi/10.1177/1528083716679157.

Rayyaan, R., W.R. Kennon, P. Potluri, and M. Akonda. 2020. Fibre Architecture Modification to Improve the Tensile Properties of Flax-Reinforced Composites. *Journal of Composite Materials* 54, no. 3 (February 1): 379–395. https://doi.org/10.1177/0021998319863156.

Sepe, R., F. Bollino, L. Boccarusso, and F. Caputo. 2018. Influence of Chemical Treatments on Mechanical Properties of Hemp Fiber Reinforced Composites. *Composites Part B: Engineering* 133, no. Supplement C (January 15): 210–217. http://www.sciencedirect.com/science/article/pii/S1359836817327919.

Shah, D.U. 2014. Natural Fibre Composites: Comprehensive Ashby-Type Materials Selection Charts. *Materials & Design (1980-2015)* 62 (October 1): 21–31. http://www.sciencedirect.com/science/article/pii/S0261306914003641.

Shah, D.U., P.J. Schubel, and M.J. Clifford. 2013. Modelling the Effect of Yarn Twist on the Tensile Strength of Unidirectional Plant Fibre Yarn Composites. *Journal of Composite Materials* 47, no. 4 (February 1): 425–436. https://doi.org/10.1177/0021998312440737.

Shahzad, A. 2012. Hemp Fiber and Its Composites – a Review. *Journal of Composite Materials* 46, no. 8 (April 1): 973–986. https://doi.org/10.1177/0021998311413623.

Torres, J.P., L.-J. Vandi, M. Veidt, and M.T. Heitzmann. 2017. The Mechanical Properties of Natural Fibre Composite Laminates: A Statistical Study. *Composites Part A: Applied Science and Manufacturing* 98, no. Supplement C (July 1): 99–104. http://www.sciencedirect.com/science/article/pii/S1359835X17301136.